Reduced acquisition time for thallium myocardial perfusion imaging with large field cadmium-zinc-telluride SPECT/CT cameras: An equivalence study

P. B. Bonnefoy, MD, MS,[a,b,e] L. Janvier, MD,[a] C. Arede, MD,[a] C. Drouet, MD,[a,c] D. Harami, MS,[a] S. Marque, MS,[d] and R. Ahond-Vionnet, MD[a]

[a] Service de Médecine Nucléaire, Hôpital Pierre Bérégovoy, Nevers, France
[b] Service de Médecine Nucléaire, CHU Saint-Etienne - Hôpital Nord, Saint Etienne, France
[c] Service de Médecine Nucléaire, Centre Georges-François Leclerc, Dijon, France
[d] Société CAPIONIS, Bordeaux, France
[e] Service de Médecine Nucléaire, CHU de Saint-Etienne, Saint-Étienne, France

Received Aug 6, 2020; accepted Mar 3, 2021
doi:10.1007/s12350-021-02611-z

Background. **Cadmium-zinc-telluride (CZT) SPECT/CT cameras with large field of view offer a higher sensitivity than conventional Anger cameras. This prospective study aimed to determine the equivalence between a conventional protocol and a reduced acquisition time protocol for 201-Thallium myocardial perfusion imaging (MPI) using a whole-body CZT SPECT camera.**

Methods and Results. **Stress MPI was obtained for 103 consecutive patients on a DISCOVERY-CZT camera. Images were anonymized and post-processed to simulate a 25% (D75 dataset) and 50% (D50 dataset) decrease in total recorded counts. Concerning the number of segments displaying a tracer uptake < 70% of maximum intensity per patient, equivalence was demonstrated for both count-reduced datasets with a good inter-observer agreement (between 0.90 and 0.88). When comparing the full-vs-D75 datasets and full-vs-D50 datasets, mean difference was 0.06 segment (CI95: [− 0.15;0.27], $P < 0.001$) and 0.518 segment (CI95: [0.28;0.76], $P < 0.001$) respectively. Inter-observer agreement was also moderate to good concerning the number of pathological segments (between 0.6 and 0.7) and excellent for functional parameters.**

Conclusion. **Whole-body CZT SPECT/CT cameras allow to reduce 201-Thallium MPI injected activity or acquisition time by 50% with an equivalence in the number of segments displaying a tracer uptake < 70% of maximum intensity and with a good inter-observer agreement. (J Nucl Cardiol 2022;29:1933–41.)**

Key Words: Cadmium-zinc-telluride • SPECT • myocardial perfusion imaging • ^{201}Thallium

Supplementary Information The online version contains supplementary material available at https://doi.org/10.1007/s12350-021-02611-z.

The authors of this article have provided a PowerPoint file, available for download at SpringerLink, which summarizes the contents of the paper and is free for re-use at meetings and presentations. Search for the article DOI on SpringerLink.com.

The authors have also provided an audio summary of the article, which is available to download as ESM, or to listen to via the JNC/ASNC Podcast.

Funding None.

Reprint requests: P. B. Bonnefoy, MD, MS, Service de Médecine Nucléaire, CHU de Saint-Etienne, 42055 Saint-Étienne, France; *p.benoit.bonnefoy@chu-st-etienne.fr*

1071-3581/$34.00

Abbreviations	
MPI	Myocardial perfusion imaging
SPECT	Single-photon emission computed tomography
D75	Dataset containing 75% of original dataset counts
D50	Dataset containing 50% of original dataset counts
IHD	Ischemic heart disease
CZT	Cadmium-zinc-telluride
FBP	Filtered back projection
EDV	End-diastolic volume
ESV	End-systolic volume
EF	Ejection fraction
CCC	Concordance correlation coefficient
CTAC	Computed tomographic attenuation correction

See related editorial, pp. 1942–1945

AIM

Cardiovascular diseases represent the first cause of death in Europe and worldwide.[1] Myocardial perfusion imaging (MPI) with single-photon emission computed tomography (SPECT) plays a major role in the screening and follow-up of patients suffering from ischemic heart disease (IHD). This imaging modality is well validated and a negative stress MPI identifies subjects at low risk of future cardiovascular events.[2]

In the last decade, dedicated cadmium-zinc-telluride (CZT) cameras brought a new advance in nuclear cardiology, offering higher sensitivity and better spatial and energy resolution than Anger cameras[3] while holding the same negative predictive value.[4] These dedicated cameras allow for a reduction in acquisition time and/or in injected radiopharmaceutical activity without compromising image quality.[5–8] Recently, CZT detector technology has been expanded to dual head SPECT cameras for whole-body imaging. These cameras with parallel collimators can be used for a wide range of scintigraphic examinations with faster acquisitions,[9–14] which could lead to their development. The feasibility of myocardial perfusion SPECT imaging using the new whole-body General Electric Discovery NM 670 CZT camera was reported with technetium-99m labeled tracers[15,16] but there is still a need for standardization of acquisition and reconstruction parameters.

As with dedicated CZT camera,[17] we hypothesized that dose or time reduction is also achievable with whole-body SPECT cameras without compromising image quality. This study aimed to determine the equivalence between a conventional protocol of MPI performed with ^{201}Thallium on a CZT SPECT/CT camera, and a reduced acquisition time protocol simulated by list-mode edition.

MATERIALS AND METHODS

Design

This monocentric trial prospectively included consecutive patients performing a MPI in our center from December 2017 to March 2018. The study was approved by the local Ethical Committee and conformed to the Declaration of Helsinki on human research. Written informed consent was obtained from every patient after complete explanation of the protocol.

Stress Protocol and Image Acquisition

Exercise stress testing was performed on a bicycle ergometer up to 85% of age-predicted maximal heart rate before intravenous infusion of 1.5 MBq kg^{-1} of ^{201}Thallium. For patients who could not sustain physical exercise, a pharmacologic stress was performed with an intravenous infusion of 0.7 mg kg^{-1} of dipyridamole (with a maximum dose of 63 mg). All stress tests were performed under 12-lead electrocardiogram monitoring with serial blood pressure measurement. All images were recorded in list mode on a DISCOVERY NM 670 CZT camera (GE Healthcare) within a maximum of 10 minutes after the injection of ^{201}Thallium (50 s/projection, 32 projections).

Post-processing

First, native data were anonymized with ''Anonymized Export'', a dedicated program available on Xeleris 4.0 stations (GE Healthcare). Anonymization was performed by a Nuclear Medicine physician subsequently not involved in images analysis (CA). After anonymization, data were post-processed by the same physician to decrease the total recorded counts by 25% or 50% (simulating a reduction of 25% or 50% in the acquisition time), thus generating D75 and D50 datasets, respectively.

Images were reconstructed by filtered back projection (FBP) with QGS/QPS software on a Xeleris 4.0 station (GE Healthcare), using a Butterworth filter with cutting frequency set to 0.4 and power set to 10 and a quantitative ramp filter. Images were manually reoriented by each reader during analysis and a motion correction was applied if necessary. Correction attenuation was not performed.

Stress images were analyzed with QGS/QPS software by three different readers (PBB, LJ, RAV) blinded for post-processing and clinical information. Each reader had access to all functions of the software to study perfusion (including multiplanar images with various color scales and normalized polar maps with a 17-segment LV model) and function on gated images. A qualitative and semi-quantitative analysis was performed. Qualitative interpretation was based on the experience of the three readers to determine the number of

segments considered to be pathological. For example, in case of perfusion abnormalities, data obtained from ECG-gated images helped to distinguish true perfusion defects from artifacts. Semi-quantitative analysis expressed segmental tracer uptake on stress scans as a percentage of maximum myocardial tracer uptake. This analysis aimed to identify segments displaying a tracer uptake lower than 70% of the maximum. LV function analysis was performed from 16 frames ECG-gated images with an automatic calculation of end-diastolic volume (EDV), end-systolic volume (ESV) and ejection fraction (EF).

Statistical Analysis

The main outcome was to assess the equivalence between datasets (full dataset, D75 and D50) concerning the number of segments displaying an uptake lower than 70% of the maximum myocardial uptake.

Secondary outcomes included the assessment of equivalence between datasets concerning the number of segments considered to be pathological and the values of functional parameters (EF, EDV and ESV) derived from ECG-gated images. Finally, we also evaluated inter-observer agreement in interpretation, based on the number of segments considered as pathological and for functional parameters.

Equivalence was demonstrated if the CI95 of the difference fell within equivalence margins, set to 1 segment. Multiple testing was addressed using a hierarchical gatekeeping procedure. Agreement between the 3 readers was assessed by the Lin's CCC (Concordance Correlation Coefficient).

RESULTS

During the study period, 103 consecutive patients with complete stress MPI were included. The description of the population is summarized in Table 1.

Segmental perfusion and functional parameters have shown a good concordance between the three datasets both for normal and pathological cases, as illustrated in Figures 1 and 2. The average number of segments identified per patient as displaying a tracer uptake lower than 70% of the maximum myocardial uptake was 6.0, 6.0 and 6.5 for the full, D75 and D50 datasets respectively (range was 0-14 for the 3 datasets). The mean number of segments considered pathological per patient was 0.8, 0.8 and 0.9 (range 0-8), respectively. Mean FE was 68.5%, 68.9% and 67.8% respectively (Table 2).

Considering our principal outcome, equivalence in the number of segments displaying a tracer uptake lower than 70% of the maximum myocardial uptake was demonstrated for both count-reduced datasets (Table 3A). Comparison between full dataset and D75 yielded a mean difference of 0.06 (CI 95 [− 0.15;0.27]), and with our pre-defined equivalence margin of 1 segment, the associated *P*-value was < 0.001. Regarding the full versus D50 datasets comparison, mean difference was 0.518 (CI 95 [0.28;0.76]) and the associated *P*-value < 0.001. Agreement between readers was good concerning the number of segments displaying a tracer

Table 1. Clinical characteristics of the population

Clinical characteristics		
Age (years)	Mean (SD)	66.5 (11.4)
Gender	M/F ratio	1.23
Weight (kg)	Mean (SD)	79.4 (17.0)
Risk factors		
Age > 55 years	N (%)	84 (81.6%)
Diabetes	N (%)	34 (33.0%)
Systolic hypertension	N (%)	68 (66.0%)
Dyslipidemia	N (%)	52 (50.5%)
Smoking or cessation < 3 months	N (%)	29 (28.2%)
Coronary heredity	N (%)	36 (35.0%)
Cumulative risk factor	Mean (SD)	3.5 (1.3)
	Min; Max	1; 6
Cardiovascular disease		
Coronaropathy	N (%)	40 (38.8%)
Ischemia	N (%)	31 (30.1%)
Necrosis	N (%)	1 (1.0%)
Total number of patients	N (%)	103 (100%)

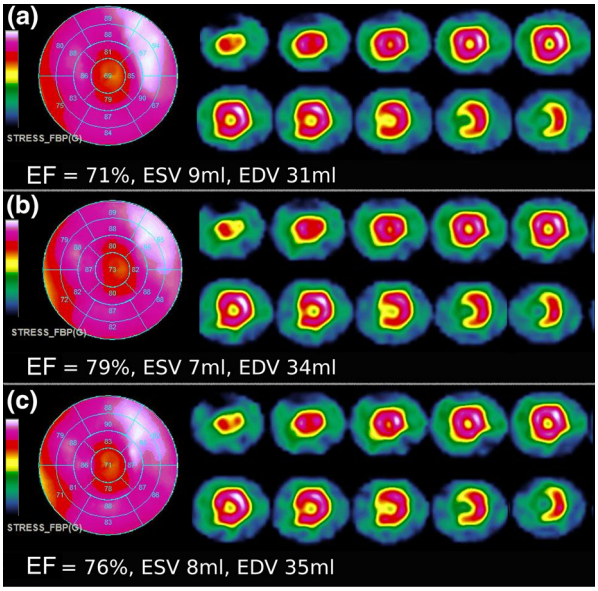

Figure 1. Clinical illustration of a normal post-stress myocardial perfusion SPECT (bullseye and short axis). No pathological segment was found, irrespective of the dataset used: full set (**a**) reduced to 75% (**b**) and reduced to 50% of total counts (**c**). EF value and myocardial volumes show limited variations. *EF*, ejection fraction; *ESV*, end-systolic volume; *EDV*, end-diastolic volume.

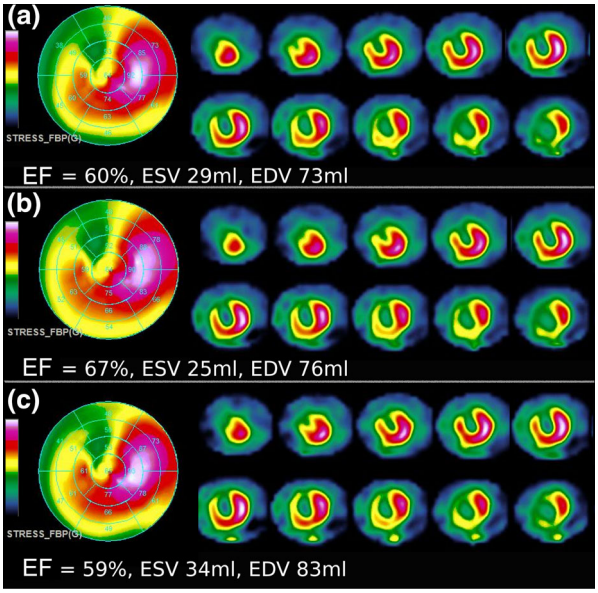

Figure 2. Clinical illustration of pathological post-stress myocardial perfusion SPECT (bullseye and short axis). Pathological segments appear identical whatever dataset is used: full set (**a**) reduced to 75% (**b**) and reduced to 50 % of total counts (**c**). EF value and myocardial volumes show limited variations. We can observe an increased visualization of digestive activity after a 50% reduction of total counts in comparison with other datasets. *EF*, ejection fraction; *ESV*, end-systolic volume; *EDV*, end-diastolic volume.

uptake lower than 70% of the maximum myocardial uptake, with a CCC = 0.90 for full dataset, 0.89 for D75 and 0.88 for D50 (Table 4).

Equivalence was also demonstrated for both count-reduced datasets concerning the number of segments considered to be pathological per patient (Table 3B). Comparison between full dataset and D75 yielded a mean difference of 0.003 (CI 95 [− 0.07;0.06]) which, considering an equivalence margin of 1 segment, led to a *P*-value < 0.001. Regarding the full versus D50 datasets comparison, mean difference was 0.147 (CI 95 [0.03;0.27]) and the associated *P*-value was < 0.001. Agreement between observers was moderate relating to the number of segments identified as pathological (between 0.6 and 0.7)

Agreement between readers was excellent for EF (0.97, 0.96 and 0.97 for full dataset, D75 and D50, respectively), EDV (0.98, 0.75 and 0.98 respectively) and ESV (0.99, 0.82 and 0.97 respectively).

DISCUSSION

Our results, obtained in a prospective cohort of consecutive patients referred for a ^{201}Tl stress MPI, confirm that a reduction in dose or acquisition time is possible with novel whole-body CZT SPECT/CT cameras. We demonstrated that, up to a reduction of 50% in total recorded counts, the number of segments displaying a tracer uptake lower than 70% of the maximum myocardial uptake is equivalent to that obtained with our standard acquisition protocol. This equivalence remains true for the number of segments considered pathological, and for functional parameters such as EF and LV volumes.

In our study, the agreement between the 3 readers, blinded from post-processing parameters, was excellent for quantitative and semi-quantitative variables including the number of segments displaying a tracer uptake lower than 70% of the maximum myocardial uptake, EF, EDV or ESV. Inter-observer agreement for more subjective variables such as the number of segments considered pathological is lower but still remains satisfying.

These data are consistent with the literature. A moderate inter-observer variability has already been reported for MPI by Johansen et al[18] They reported moderate to good inter-observer agreement (κ = 0.52-0.56) for segmental score interpretation in a cohort of 108 consecutive male patients with stable angina pectoris.

Moreover, our results fit with data obtained initially on dedicated cardiac CZT cameras. In a cohort of 10 patients undergoing stress MPI acquired with a dedicated CZT SPECT camera, Palyo et al reported no

Table 2. MPI results according to the post-processing protocol

Variable	Protocol		
	100%	75%	50%
Number of patients analyzed			
n (m.d.)	100 (3)	100 (3)	102 (1)
Number of segments displaying a tracer uptake < 70% of the maximum myocardial uptake, per patient			
Mean (SD)	6.0 (3.2)	6.0 (3.3)	6.5 (3.2)
Median (Q1; Q3)	6 (4; 9)	6 (4; 9)	6 (4; 9)
Min; Max	0; 14	0; 14	0; 14
Number of segments considered pathological per patient			
Mean (SD)	0.8 (1.5)	0.8 (1.6)	0.9 (1.6)
Median (Q1; Q3)	0 (0; 1)	0 (0; 1)	0 (0; 1)
Min; Max	0; 8	0; 8	0; 8
EF			
Mean (SD)	68.5 (15.7)	68.9 (15.4)	67.8 (15.6)
Median (Q1; Q3)	72 (62; 79)	72 (63; 80)	70 (60; 78)
Min; Max	16; 95	18; 97	13; 94
EDV			
Mean (SD)	68.7 (40.7)	72.2 (43.0)	72.4 (40.2)
Median (Q1; Q3)	59 (42; 81)	61 (45; 84)	62 (46; 85)
Min; Max	24; 283	25; 295	24; 269
ESV			
Mean (SD)	26.8 (33.9)	28.3 (36.2)	28.4 (33.9)
Median (Q1; Q3)	17 (9; 30)	17 (11; 31)	20 (11; 34)
Min; Max	1; 237	1; 242	2; 234

m.d. missing data due to acquisition artifacts or technical issues which made post-processing impossible

differences in the size of regional defects, LV volume, or ejection fraction with a 50% reduction protocol.[17] Reduction in the acquisition time or in the injected activity is an important benefit for nuclear imaging techniques. By reducing the acquisition time, the comfort of the patient is improved, leading to reduced motion artifacts and better image quality. Reducing the injected activity lowers the dose delivered to the patient, which seems particularly interesting when using ^{201}Tl for MPI.

Ultra-low-dose protocols are currently validated with technetium-99m labeled radiotracers on dedicated CZT SPECT cameras (injection of 1.85 MBq/kg leading to an effective dose < 1 mSv) with good sensitivity.[19] The high negative predictive value of normal MPI using an ultra-low-dose protocol was also established both with technetiated radiotracers and thallium.[4,20] However, artifacts are often seen with Anger and dedicated CZT cameras and lead to a reduction in the specificity of the examination.[19] Attenuation artifacts were frequent in our cohort. The variable ''Number of segments < 70% of maximal intensity'' reported all segments with significantly altered tracer uptake, possibly due to a true perfusion defect or an artifact. The variable ''Number of segments considered pathological'' results from qualitative analysis including the information given by ECG-gated data and is somewhat more dependent on the experience of the reader. As attenuation correction was not applied, the average number of segments lower than 70% is high, but the number of segments considered

Table 3. Results for equivalence tests

(A) Equivalence analysis: Main outcome—number of segments displaying a tracer uptake < 70% of the maximum myocardial uptake, per patient

Protocol		
Difference 75%–100%	n (m.d.)	99 (4)
	Mean (SD)	0.061 (1.05)
	Median (Q1; Q3)	0 (− 1; 0)
	Min; Max	-3; 4
Equivalence test results (equivalence interval: [− 1; 1])		
	IC95%	[− 0.15; 0.27]
	P-value*	< 0.001
Difference 50%–100%	n (m.d.)	100 (3)
	Mean (SD)	0.518 (1.20)
	Median (Q1; Q3)	0 (0; 1)
	Min; Max	-2; 4
Equivalence test results (equivalence interval: [− 1; 1])		
	IC95%	[0.28; 0.76]
	P-value*	< 0.001

(B) Equivalence analysis: Secondary outcome—Number of segments considered pathological per patient

Protocol		**Total**
Difference 75%–100%	n (m.d.)	99 (4)
	Mean (SD)	− 0.003 (0.31)
	Median (Q1; Q3)	0 (0; 0)
	Min; Max	− 1; 2
Equivalence test results (equivalence interval: [− 1; 1])		
	IC95%	[− 0.07; 0.06]
	P-value*	< 0.001
Difference 50%–100%	n (m.d.)	100 (3)
	Mean (SD)	0.147 (0.61)
	Median (Q1; Q3)	0 (0; 0)
	Min; Max	− 2; 3
Equivalence test results (equivalence interval: [− 1; 1])		
	IC95%	[0.03; 0.27]
	P-value*	< 0.001

**P*-value for paired t test
m.d. missing data due to acquisition artifacts or technical issues which made post-processing impossible

pathological by readers was much lower (respectively 0.8, 0.8 and 0.9 for the 3 datasets), suggesting a high prevalence of attenuation artifacts. However, the ability of the readers to identify these artifacts was not impacted by the reduction in the total number of counts, as demonstrated by a stable number of segments considered pathological across the three datasets.

A recent meta-analysis reported good diagnostic performance in detecting angiographically proven coronary artery disease for both conventional SPECT (pooled sensitivity and specificity 85% and 66% respectively) and for CZT SPECT (pooled sensitivity and specificity 89% and 69% respectively), with a slightly higher accuracy for CZT SPECT.[21] Computed tomography-based attenuation correction (CTAC), available with the majority of Anger cameras but only with a minority of dedicated cardiac CZT cameras, is a useful method to improve specificity. As for Anger cameras,

Table 4. Evaluation of concordance with Lin Concordance Coefficients (CCC)

Variable/protocol	n	CCC	IC95%
Number of segments < 70% of maximal intensity per patient			
100%	99	0.896	[0.863;0.929]
75%	100	0.893	[0.860;0.927]
50%	99	0.880	[0.842;0.918]
Number of segments considered pathological per patient			
100%	98	0.691	[0.613;0.769]
75%	100	0.706	[0.631;0.781]
50%	101	0.629	[0.541;0.716]
EF			
100%	99	0.974	[0.966;0.983]
75%	100	0.958	[0.944;0.972]
50%	101	0.967	[0.955;0.978]
EDV			
100%	99	0.986	[0.981;0.990]
75%	100	0.752	[0.681;0.822]
50%	101	0.980	[0.973;0.986]
ESV			
100%	99	0.995	[0.994;0.997]
75%	100	0.821	[0.767;0.875]
50%	101	0.973	[0.964;0.982]

whole-body CZT SPECT cameras are mainly equipped with CT, allowing for CTAC with a potential increase in specificity. Moreover, CT images can provide an evaluation of the coronary calcium score[22] which brings a complementary appreciation of the cardiovascular risk.[23]

Our study has some limitations. First, our main outcome was based on protocol optimization and image quality evaluation, thus only stress acquisitions were analyzed and patient outcome was not available. A longitudinal study with clinical follow-up is needed to evaluate the performances of these new devices in terms of cardiovascular events risk prediction. Second, data were missing for three patients due to acquisition artifacts or technical issues which made post-processing impossible. Third, intra-observer variability was not evaluated in our study. We chose to focus on inter-observer variability because it is the most penalizing situation in clinical routine. Finally, this study focused only on a ^{201}Thallium imaging protocol. Dedicated evaluations are necessary for technetium-99m labeled tracers and some data are already available in literature.[15,16] Recently, Morelle et al[15] reported the first comparison of performances between the new whole-body CZT SPECT/CT camera and a dedicated cardiac CZT camera for myocardial perfusion imaging using ^{99m}Tc-sestamibi. They reported a slightly poorer spatial resolution of whole-body CZT SPECT/CT camera (DNM 670CZT, GE Healthcare) compared with dedicated cardiac CZT SPECT camera (DNM 530c, GE Healthcare). Despite this difference, results obtained in patients were concordant between both cameras in terms of perfusion, EDV, ESV, EF, wall motion and thickening scores. In 19 patients that underwent sequential low-dose ^{99m}Tc-tetrofosmin both on dedicated cardiac CZT camera and whole-body CZT SPECT/CT camera, Gimelli et al[16] also reported an excellent correlation for segmental myocardial uptake. To the best of our knowledge, our study is the first to address the impact of a reduction in acquisition time or injected activity when using ^{201}Thallium for MPI on a whole-body CZT camera.

NEW KNOWLEDGE GAINED

The current study highlights the validity of whole-body CZT SPECT/CT thallium myocardial perfusion imaging in clinical routine and demonstrates the possibility to reduce injected activity or acquisition time with

equivalent image interpretation compared to a standard protocol.

CONCLUSION

Novel whole-body CZT SPECT/CT cameras allow to adapt protocols designed for Anger cameras in order to reduce injected activity or acquisition time by 50% while maintaining equivalent image interpretation and a good inter-observer agreement.

Acknowledgements

Authors want to warmly thank Ms. Stéphanie PERNES for her Substantial contributions to the acquisition of clinical data.

Disclosures

RAV and LJ reported Support for travel to meetings for the study. Others authors declare they have no conflict of interest.

References

1. Naghavi M, Wang H, Lozano R, et al. Global, regional, and national age-sex specific all-cause and cause-specific mortality for 240 causes of death, 1990-2013: A systematic analysis for the Global Burden of Disease Study 2013. Lancet 2015;385:117-71. https://doi.org/10.1016/S0140-6736(14)61682-2.
2. Pavin D, Delonca J, Siegenthaler M, et al. Long-term (10 years) prognostic value of a normal thallium-201 myocardial exercise scintigraphy in patients with coronary artery disease documented by angiography. Eur Heart J 1997;18:69-77. https://doi.org/10.1093/oxfordjournals.eurheartj.a015120.
3. Takahashi Y, Miyagawa M, Nishiyama Y, et al. Performance of a semiconductor SPECT system: Comparison with a conventional Anger-type SPECT instrument. Ann Nucl Med 2013;27:11-6. https://doi.org/10.1007/s12149-012-0653-9.
4. Songy B, Guernou M, Hivoux D, et al. Prognostic value of one millisievert exercise myocardial perfusion imaging in patients without known coronary artery disease. J Nucl Cardiol 2016;25:120-30. https://doi.org/10.1007/s12350-016-0601-5.
5. Einstein AJ, Blankstein R, Andrews H, et al. Comparison of image quality, myocardial perfusion, and left ventricular function between standard imaging and single-injection ultra-low-dose imaging using a high-efficiency spect camera: The MILLI-SIEVERT study. J Nucl Med 2014;55:1430-7. https://doi.org/10.2967/jnumed.114.138222.
6. Verger A, Djaballah W, Fourquet N, et al. Comparison between stress myocardial perfusion SPECT recorded with cadmium-zinc-telluride and Anger cameras in various study protocols. Eur J Nucl Med Mol Imaging 2012. https://doi.org/10.1007/s00259-012-2292-8.
7. Imbert L, Poussier S, Franken PR, et al. Compared performance of high-sensitivity cameras dedicated to myocardial perfusion SPECT: A comprehensive analysis of phantom and human images. J Nucl Med 2012;53:1897-903. https://doi.org/10.2967/jnumed.112.107417.
8. Esteves FP, Raggi P, Folks RD, et al. Novel solid-state-detector dedicated cardiac camera for fast myocardial perfusion imaging: Multicenter comparison with standard dual detector cameras. J Nucl Cardiol 2009;16:927-34. https://doi.org/10.1007/s12350-009-9137-2.
9. Sadr AB, Testart N, Tylski P, Scheiber C. Reduced scan time in 123 I-FP-CIT SPECT imaging using a large-field cadmium-zinc-telluride camera. Clin Nucl Med 2019;44:568-9. https://doi.org/10.1097/RLU.0000000000002554.
10. Melki S, Chawki MB, Marie P, et al. Augmented planar bone scintigraphy obtained from a whole-body SPECT recording of less than 20 min with a high-sensitivity 360C ZT camera. Eur J Nucl Med Mol Imaging 2020;47:1329-31.
11. Okano N, Osawa I, Tsuchihashi S, et al. High-speed scanning of planar images showing 123 I-MIBG uptake using a whole- body CZT camera: A phantom and clinical study. EJNMMI Res 2019;9:1-10.
12. Bordonnea M, Mariea P-Y, Imbert L, Verger A. Brain perfusion SPECT acquired using a dedicated brain configuration on a 360° whole-body CZT-camera. J Neuroradiol 2020;47:180-1. https://doi.org/10.1016/j.neurad.2019.11.002.
13. Bellevre D, Bailliez A, Blaire T, et al. Quantitation of myocardial 99m Tc-HMDP uptake with new SPECT/CT cadmium zinc telluride (CZT) camera in patients with transthyretin-related cardiac amyloidosis: Ready for clinical use? J Nucl Cardiol 2020. https://doi.org/10.1007/s12350-020-02274-2.
14. Desmonts C, Bouthiba MA, Enilorac B, et al. Evaluation of a new multipurpose whole- body CzT-based camera: Comparison with a dual-head Anger camera and first clinical images. EJNMMI Phys 2020;7:1-16.
15. Morelle M, Bellevre D, Hossein-Foucher C, et al. First comparison of performances between the new whole-body cadmium-zinc-telluride SPECT-CT camera and a dedicated cardiac CZT camera for myocardial perfusion imaging: Analysis of phantom and patients. J Nucl Cardiol 2019. https://doi.org/10.1007/s12350-019-01702-2.
16. Gimelli A, Liga R, Bertasi M, et al. Head-to-head comparison of a CZT-based all-purpose SPECT camera and a dedicated CZT cardiac device for myocardial perfusion and functional analysis. J Nucl Cardiol 2019. https://doi.org/10.1007/s12350-019-01835-4.
17. Palyo RJ, Sinusas AJ, Liu Y-H. High-sensitivity and high-resolution SPECT/CT systems provide substantial dose reduction without compromising quantitative precision for assessment of myocardial perfusion and function. J Nucl Med 2016;57:893-9.
18. Johansen A, Gaster AL, Veje A, et al. Interpretive intra- and interobserver reproducibility of rest/stress Tcm-sestamibi myocardial perfusion SPECT in a consecutive group of male patients with stable angina pectoris before and after percutaneous transluminal angioplasty. Nucl Med Commun 2001;22:531-7. https://doi.org/10.1097/00006231-200105000-00011.
19. Fiechter M, Ghadri JR, Kuest SM, et al. Nuclear myocardial perfusion imaging with a novel cadmium-zinc-telluride detector SPECT/CT device: First validation versus invasive coronary angiography. Eur J Nucl Med Mol Imaging 2011;38:2025-30. https://doi.org/10.1007/s00259-011-1877-y.
20. Bednárová V, Kincl V, Kamínek M, et al. The prognostic value of ultra low-dose thallium myocardial perfusion protocol using CZT SPECT. Int J Cardiovasc Imaging 2019;35:1163-7. https://doi.org/10.1007/s10554-019-01535-7.
21. Cantoni V, Green R, Acampa W, et al. Diagnostic performance of myocardial perfusion imaging with conventional and CZT single-photon emission computed tomography in detecting coronary artery disease: A meta-analysis. J Nucl Cardiol 2019. https://doi.org/10.1007/s12350-019-01747-3.

22. Einstein AJ, Johnson LL, Bokhari S, et al. Agreement of visual estimation of coronary artery calcium from low-dose CT attenuation correction scans in hybrid PET/CT and SPECT/CT with standard agatston score. J Am Coll Cardiol 2010;56:1914-21. https://doi.org/10.1016/j.jacc.2010.05.057.
23. Chang SM, Nabi F, Xu J, et al. The coronary artery calcium score and stress myocardial perfusion imaging provide independent and complementary prediction of cardiac risk. J Am Coll Cardiol 2009;54:1872-82. https://doi.org/10.1016/j.jacc.2009.05.071.